

# Effect of the ratio of solid to liquid conductivity on the stability parameter of dendrites within a phase-field model of solidification

A. M. Mullis

*Institute for Materials Research, University of Leeds, Leeds LS2 9JT, United Kingdom*

(Received 14 March 2003; published 11 July 2003)

We use a phase-field model of dendritic growth in a pure undercooled melt to examine the effect of the ratio  $\mu = \kappa_s / \kappa_l$  on the operating point of the needle crystal and hence the stability parameter  $\sigma^*$ , where  $\kappa_s$  and  $\kappa_l$  are the thermal conductivities of the solid and liquid phases, respectively. These results are compared with the microscopic solvability calculations of Barbieri and Langer [Phys. Rev. A **39**, 5314 (1989)]. We find that in our phase-field model  $\sigma^*$  varies much more rapidly with  $\mu$  than is predicted from solvability theory.

DOI: 10.1103/PhysRevE.68.011602

PACS number(s): 68.70.+w, 81.30.-t, 64.10.+h

## I. INTRODUCTION

One of the most fundamental and all-pervasive microstructures produced during the solidification of metals is the dendrite. Dendrites are crystals that develop complex, time dependent shapes, normally as the result of extensive branching which gives rise to a treelike structure. In recent years the complex patterns produced by growing dendrites have been a source of immense theoretical interest. The dendrite is a prime example of a pattern forming system where complex morphologies arise from initially homogeneous conditions due to the highly nonlinear response of the controlling system. Although the governing equations for dendritic growth have been known for many decades, finding solutions to the free-boundary problem, even in the tip region, has proved enormously complicated.

Dendritic growth is also important from an engineering viewpoint. Remnants of dendritic microstructures often survive subsequent processing operations, such as rolling and forging, and the length scales established by the dendrite can influence not only the final grain size but also micro- and hence macrosegregation patterns. This can have a wide-ranging influence on both the properties of finished metallic products, affecting, for instance, mechanical properties, corrosion resistance, and surface finish, and the formability of metallic feedstock, such as the ability to resist hot tearing during rolling.

Where dendritic growth has been observed directly, in transparent analog casting systems such as succinonitrile [1] and xenon [2], the evidence is that the morphology of dendrites grown at different undercoolings is probably self-similar when scaled against the tip radius  $R$ . Consequently, all the more obvious length scales of the dendrite are simple multiples of  $R$ , making the ability to predict  $R$  accurately a problem of central importance to the theory of dendritic growth.

The first mathematical model of dendritic growth was provided by Ivantsov [3], who showed that an isothermal paraboloid of revolution with radius of curvature  $R$  at the tip, growing at velocity  $V$  into an undercooled melt, was a shape preserving solution to the diffusion equation, thus giving rise to the idea of the parabolic needle dendrite. The analytical solution for such a crystal growing into its undercooled melt

is degenerate, in that it relates the Péclet number, and not the growth velocity, to undercooling, where the Péclet number is defined as

$$\text{Pe} = \frac{VR}{2a_1} \quad (1)$$

with  $a_1$  being the thermal diffusivity in the melt. Consequently, at a given undercooling an infinite set of solutions are admissible, subject to the condition  $VR = \text{const}$ . Such degeneracy is not observed in nature, where a well-defined growth velocity can always be associated with a given undercooling.

In recent years the theory of microscopic solvability [4,5] has provided a plausible mechanism for the selection of  $R$ . The principal physical insight of solvability theory is that surface tension acts as a singular perturbation which resolves the degeneracy found in the macroscopic problem. However, the selection mechanism turns out to be beyond all orders of perturbation theory [6] and consequently rather subtle techniques need to be employed to solve the problem.

The basis of solvability theory is that Green's functions can be employed to convert the diffusion and interface continuity equations into an integro-differential equation that contains the surface energy. Perhaps counter to intuition, it turns out that in the case of an isotropic surface energy this equation has no solutions. Anisotropy can be introduced by letting

$$d_0 \rightarrow d_0(\theta) = d_0(1 + \gamma \cos k\theta) \quad (2)$$

where  $d_0$  is the thermal capillary length, defined by

$$d_0 = \frac{\sigma T_m c}{L^2}. \quad (3)$$

Here  $L$  is the latent heat per unit volume,  $c$  is the specific heat per unit volume,  $\sigma$  is the interfacial energy between the solid and liquid phases,  $T_m$  is the melting temperature,  $\gamma$  defines the anisotropy strength,  $\theta$  is the angle between the local outward pointing normal to the interface and the principal growth direction, and  $k$  is a mode number, which for

growth in a cubic metal will be 4. The principal prediction of this theory is that capillary forces break the Ivantsov degeneracy via the relationship

$$R^2V = \frac{2a_1d_0}{\sigma^*}, \quad (4)$$

where  $\sigma^*$  is the anisotropy dependent eigenvalue for the problem, which for small Péclet numbers is found to vary as  $\sigma^*(\gamma) \propto \gamma^{7/4}$ .

In recent years further progress has been made toward understanding dendritic growth by the advent of phase-field modeling [7–9]. The basis of the phase-field technique is the definition of a phase variable  $\phi(x,t)$ , which is continuous over the whole region  $\Omega$  occupied by the system,  $x$  being the spatial coordinates within  $\Omega$  and  $t$  being time. The value of  $\phi$  indicates whether the material is solid or liquid. The continuity of  $\phi$  over  $\Omega$  implies that the interface between the solid and liquid regions is diffuse, which is one of the central differences between the phase-field formulation of the dendrite growth problem and microscopic solvability. The evolution of the phase variable  $\phi$  is governed by an entropy functional which ensures the increase in entropy and which is coupled to either the temperature field  $T(x,t)$  for thermal growth or the solute concentration field  $c(x,t)$  for solutal growth.

Like solvability theory, phase-field techniques predict that in an unconstrained medium dendrites will be formed only in the presence of a nonzero crystalline anisotropy [8], although where the medium is constrained by a narrow channel this is not the case and dendrites can be formed [10,11] in a medium with isotropic properties. For growth in an unconstrained medium the tip radius  $R$  is determined by the strength of the anisotropy  $\gamma$ . Phase-field theory would thus seem a natural companion to solvability theory for probing fundamental aspects of the dendrite growth problem. Investigating the correspondence between the two approaches, though, is not trivial. The phase-field method is a diffuse interface technique, and it is found in practice that the value of  $R$  predicted depends upon the value of the interface thickness  $\delta$  assumed. Convergence with solvability theory can thus be expected only in the limit of vanishing interface width. However, as the element size  $\Delta x$  in the computational mesh is determined by the requirement that the diffuse interface be resolved ( $\Delta x < \delta$ ), using very fine interface widths can be prohibitively computationally intensive. Moreover, in many formulations of the phase-field problem, interface kinetics are a necessary component which cannot be reduced to arbitrarily low levels [8]. Consequently, the low growth velocity regime studied by solvability theory is not always accessible in phase-field modeling.

The most significant work to date in reconciling the predictions of solvability theory with phase-field modeling has been by Karma and co-workers [12–14], who have pioneered a formulation of the phase-field problem that both is efficient in the sharp interface limit and can accommodate arbitrarily slow growth (small kinetic effects). They found that for succinonitrile (small  $\gamma$ ) there was reasonable agreement between their phase-field model and solvability theory,

with the predicted value of  $\sigma^*$  being slightly higher in the phase-field model than that given by linear solvability theory. This actually leads to the phase-field model giving better agreement with experiment than solvability theory. However, for pivalic acid (large  $\gamma$ ) they found a significant variation in the value of  $\sigma^*$  predicted by the different techniques. They attribute this to the dendrite tip shape departing significantly from parabolic for high anisotropy materials. Linear solvability theory, which assumes that anisotropy acts as a small shape correction to the Ivantsov paraboloid, may not apply under these conditions. Moreover, the definition of  $R$ , and hence  $\sigma^*$ , for nonparabolic shapes is ambiguous. Nonetheless, for low anisotropy materials, which includes most metals, phase-field techniques have been demonstrated to be a valid tool for probing the tip shape and operating point of needle crystals.

Due to their complexity, solvability models are often restricted to the assumption of either symmetric or asymmetric conductivity, that is, either  $\kappa_s = \kappa_l$  or  $\kappa_s = 0$ , where  $\kappa_s$  and  $\kappa_l$  are the thermal conductivities of the solid and liquid phases, respectively. The effect of nonsymmetric conductivities in microscopic solvability has been investigated to first order by Barbieri and Langer [15], who find

$$\sigma^*(\mu) \approx \frac{2}{1+\mu} \sigma^*(\mu=1), \quad (5)$$

where  $\mu = \kappa_s / \kappa_l$ . In this paper we use a phase-field model of dendritic growth in a pure undercooled melt to probe the effect of the ratio  $\mu$  on  $\sigma^*$ .

Although  $\kappa_s = \kappa_l$  is a common assumption in the modeling of thermal dendritic growth, reduced phonon scattering in the solid phase, relative to the liquid, means that in reality  $\kappa_s > \kappa_l$  in most metallic materials. However, quantifying the ratio  $\kappa_s / \kappa_l$ , even for pure metals, is difficult due to the scarcity of thermal conductivity data for liquid metals. For solid metals at high temperature the Wiedemann-Franz-Lorenz law, that

$$\frac{\kappa}{\sigma_e T} = \frac{\pi^2 k_B^2}{3e^2} = 2.45 \times 10^{-8} \text{ W } \Omega \text{ K}^{-1} \quad (6)$$

for all metals, is generally a reasonable approximation, where  $\sigma_e$  is the electrical conductivity. A number of studies [16,17] have shown that this relationship also appears to hold for liquid metals, and consequently the ratio  $\sigma_{es} / \sigma_{el}$  may be used as a guide to  $\kappa_s / \kappa_l$ . This ratio is typically around 1.5 for many metals although the variations are quite large. Values as low as 1.05 have been reported for Fe [18,19], while Cu, Ag, and Au all have values [20] close to 2. Mn is exceptional for a metal in that  $\sigma_{es} / \sigma_{el} = 0.6$  [20]. Si and Ge show  $\sigma_{es} / \sigma_{el} \ll 1$ , although as this is due to the phase change from a semiconducting solid to a metallic liquid, electrical conductivity is probably not a good guide to thermal conductivity in these cases. Although both Si and Ge show faceted growth under conventional solidification conditions, Ge has been shown [21,22] to grow dendritically during rapid solidification due to kinetic roughening of the solid-liquid inter-

face [22]. On balance, we believe the range  $0.5 \leq \kappa_s / \kappa_l \leq 2.0$  probably covers most materials of interest.

## II. COMPUTATIONAL METHOD

For solidification of a pure material we proceed by writing the Landau-Ginzberg entropy functional:

$$F = \int_{\Omega} \left[ f(\phi, T) + \frac{1}{2} \varepsilon^2 (\nabla \phi)^2 \right] d\Omega, \quad (7)$$

where  $T(x, t)$  is the temperature and  $\varepsilon$  is a parameter that is constant for an isotropic material. The free-energy density  $f(\phi, t)$  is a double well potential with respect to  $\phi$ . Various choices for  $\phi$  have been presented; here we closely follow the model of Wheeler *et al.* [8] for the solidification of a pure undercooled melt, and the reader is directed to that paper and the work of Wang *et al.* [23] for a detailed derivation of the model. Within this model  $0 \leq \phi \leq 1$ , with  $\phi \equiv 0$  representing the pure solid and  $\phi \equiv 1$  the pure liquid.

Following Wheeler *et al.* [8] we proceed by defining a reference length scale  $w$ , typically the longest dimension of the domain  $\Omega$ , against which other lengths may be nondimensionalized. The corresponding diffusion time scale is thus  $w^2/a_l$ , allowing the definition of a nondimensional time  $\tau = ta_l/w^2$ . Finally, defining a dimensionless temperature  $u$  by  $T = T_m + u\Delta T$ , where  $\Delta T$  is the undercooling of the melt, the transport equation may be written as

$$\frac{\partial u}{\partial \tau} + \frac{1}{\Delta} p'(\phi) \frac{\partial \phi}{\partial \tau} = \nabla \cdot (\bar{a} \nabla u), \quad (8)$$

where the prime denotes differentiation of the polynomial  $p$ :

$$p(\phi) = \phi^3(10 - 15\phi + 6\phi^2). \quad (9)$$

$\bar{a}$  is the thermal diffusivity of the material, normalized to the value of that for the pure liquid, namely,

$$\bar{a} = \frac{\phi a_l + (1 - \phi) a_s}{a_l}, \quad (10)$$

and  $\Delta$  is the dimensionless undercooling,

$$\Delta = \frac{c \Delta T}{L}. \quad (11)$$

The second term on the left hand side of Eq. (8) thus represents the latent heat associated with the change of phase of the material.

The evolution of the phase field is given by

$$\frac{\bar{\varepsilon}^2}{m} \frac{\partial \phi}{\partial \tau} = \phi(1 - \phi) \left[ \phi - \frac{1}{2} + 30\bar{\varepsilon} \alpha \Delta u \phi(1 - \phi) \right] + \bar{\varepsilon}^2 \nabla^2 \phi, \quad (12)$$

where the quantities in Eq. (12) are given by Wheeler *et al.* [8] as

$$\alpha = \frac{\sqrt{2} w L^2}{12 c \sigma T_m}, \quad (13)$$

$$m = \frac{\xi \sigma T_m}{a_l L}, \quad (14)$$

and

$$\bar{\varepsilon} = \frac{\delta}{w}. \quad (15)$$

Here  $\delta$  is a parameter defining the width of the diffuse interface and  $\xi$  is the kinetic parameter.

Equations (8) and (12) represent a complete description of solidification in an isotropic system. However, it is well established from microscopic solvability theory that crystalline anisotropy plays a central role in the selection of the operating point during the growth of needle crystals [4]. Consequently, the inclusion of anisotropy is a necessary feature of the phase-field model. This is achieved by writing  $\bar{\varepsilon}$  as a function of angle. For a two-dimensional system we write

$$\bar{\varepsilon}(\theta) = \bar{\varepsilon} \eta(\theta) = \bar{\varepsilon} (1 + \gamma \cos k\theta). \quad (16)$$

Incorporating the anisotropic form of  $\bar{\varepsilon}$  given by Eq. (16) into Eq. (12) gives [8]

$$\begin{aligned} \frac{\bar{\varepsilon}^2}{m} \frac{\partial \phi}{\partial \tau} = & \phi(1 - \phi) \left[ \phi - \frac{1}{2} + 30\bar{\varepsilon} \alpha \Delta u \phi(1 - \phi) \right] \\ & - \bar{\varepsilon}^2 \frac{\partial}{\partial x} \left( \eta(\theta) \eta'(\theta) \frac{\partial \phi}{\partial y} \right) + \bar{\varepsilon}^2 \frac{\partial}{\partial y} \left( \eta(\theta) \eta'(\theta) \frac{\partial \phi}{\partial x} \right) \\ & + \bar{\varepsilon}^2 \nabla \cdot (\eta^2(\theta) \nabla \phi). \end{aligned} \quad (17)$$

Using the expression for the outward pointing normal  $\hat{\mathbf{n}}$  to the interface,

$$\hat{\mathbf{n}} = \frac{\nabla \phi}{|\nabla \phi|} = \cos \theta \hat{\mathbf{x}} + \sin \theta \hat{\mathbf{y}} \quad (18)$$

we have

$$\tan \theta = \frac{\phi_y}{\phi_x} \quad (19)$$

and, in addition,

$$\theta_x = \frac{\phi_x \phi_{xy} - \phi_y \phi_{xx}}{|\nabla \phi|^2}, \quad (20)$$

$$\theta_y = \frac{\phi_x \phi_{yy} - \phi_y \phi_{xy}}{|\nabla \phi|^2}, \quad (21)$$

which is sufficient for the evaluation of Eq. (17).

The system of differential equations represented by Eqs. (8) and (17) is solved using a standard finite difference scheme. The transport equation is solved using an alternating direct implicit scheme, which is unconditionally stable, irrespective of the time step  $\delta t$  employed. However, the phase-

TABLE I. Material parameters used in the simulations. Note that values of  $\delta$  are given for two sets of simulations. In the first the grid spacing and  $\delta$  are held fixed, in the second they are rescaled to a fixed multiple of the dendrite tip radius  $R$ .

Quantity	Symbol	Value	Units
Latent heat	$L$	$2.35 \times 10^9$	$\text{J m}^{-3}$
Specific heat	$c$	$5.42 \times 10^6$	$\text{J K}^{-1} \text{m}^{-3}$
Liquidus temperature	$T_m$	1728	K
Thermal diffusivity	$\kappa$	$1.55 \times 10^{-5}$	$\text{m}^2 \text{s}^{-1}$
Surface energy	$\sigma$	0.370	$\text{J m}^{-2}$
Surface energy anisotropy	$\gamma$	0.02	
Interface kinetic parameter	$\xi$	1.4	$\text{m s}^{-1} \text{K}^{-1}$
Interface width parameter	$\delta$	7.5 (fixed) or 0.061 $R$ (rescaled)	nm

field equation is highly nonlinear, and consequently there is no simple implicit scheme suitable for its solution. We have therefore used an explicit numerical scheme to obtain the time dependent solution to Eq. (17). This will be subject to a Courant type stability condition of the form

$$\delta t \leq \frac{(\delta x)^2}{\psi m}, \quad (22)$$

where  $\psi$  would take the value 4 for a linear equation. The nonlinear nature of Eq. (17) actually imposes a more restrictive condition on the time step, and the optimum value of  $\psi$  has been determined empirically.

This model has been used to study the behavior of  $V$  and  $R$  as a function of  $\mu$ . During the simulation the curvature  $1/R$  of the dendrite tip is evaluated along the  $x$  axis (where the proscribed anisotropy ensures that the dendrite tip does grow along the  $x$  axis). Following Wheeler *et al.* [8], this may be written as

$$\frac{1}{R} = \frac{\phi_{yy}}{\phi_x}. \quad (23)$$

The rate at which the tip advances (identified by the point of maximum curvature) is used to calculate  $V$ . The evolution of both  $V$  and  $R$  is tracked to ensure that a steady state has been obtained, and once this is the case representative values of  $V$  and  $R$  for the simulation are calculate by averaging over a minimum of 5000 time steps.

However, great care needs to be exercised in the estimation of  $R$ . Karma and Rappel [12] have argued that the diffuse solid-liquid interface assumed in phase-field models leads to a second order effect in which the modeled attachment kinetics depend upon the thickness of the interface. Moreover, Wheeler *et al.* [8] have shown that, in the phase-field model used here, the well-known equations for single phase solidification are recovered only in the asymptotic limit of a sharp interface. In order to eliminate effects due to interface thickness as far as possible, and ensure direct comparability between simulations, the following procedure has been adopted. For each value of  $\mu$  an initial run is conducted to determine an approximate value of  $R$ . All these initial runs are performed using the same grid size and interface thick-

ness. The computational mesh and the interface width are then rescaled such that a second set of simulations is generated in which the mesh size and interface width are a constant multiple of the tip radius  $R$ . This second set of simulations is thus fully self-similar. In the results presented below the plotted error bars indicate the magnitude of the discrepancy between the values obtained using the two procedures outlined above. Only effects that show the same qualitative behavior in both data sets are described.

### III. RESULTS AND DISCUSSION

The absence of kinetic effects in the solvability model of Barbieri and Langer [15] means that their results will generally only be valid in the limit of vanishing Péclet numbers. Although solvability models have been formulated that incorporate kinetic effects, as far as we are aware no formulation exists that includes both interface kinetics and nonsymmetric conductivities. However, interface kinetics are a necessary part of our phase-field model, and consequently, although a comparison can be made for small Péclet number, these are still of necessity finite. In fact in this study the effect of  $\mu$  on  $\sigma^*$  has been studied in detail at two values of undercooling,  $\Delta T = 150$  K ( $\Delta = 0.34$ ) and  $\Delta T = 350$  K ( $\Delta = 0.80$ ). These correspond to Péclet numbers (calculated at  $\mu = 1$ ) of  $\text{Pe} \approx 0.02$  and  $\text{Pe} \approx 0.10$ , respectively. The first of these is in the regime where interface kinetics will be weak and consequently the predictions of solvability theory might be expected to be approximately valid. However, for the material parameters used here, values for which are given in Table I, the higher value of  $\text{Pe}$  corresponds to the case in which interface kinetics cannot be considered negligible [24], and consequently greater departures from the predictions of solvability theory might be expected.

The predicted variation of  $\sigma^*$  as a function of  $\mu$  in these two cases is shown in Fig. 1. As some variation of  $\sigma^*$  with  $\Delta$  is to be expected, and in order to plot both data sets on the same axes, each data set has been normalized against the appropriate value of  $\sigma^*(\mu = 1)$ . Also shown is a solid line representing the expected variation of  $\sigma^*$  with  $\mu$  as predicted by solvability theory and given by Eq. (5). From Fig. 1 it is apparent that, although in both cases the variation of  $\sigma^*$  with  $\mu$  is in the same sense as predicted by solvability

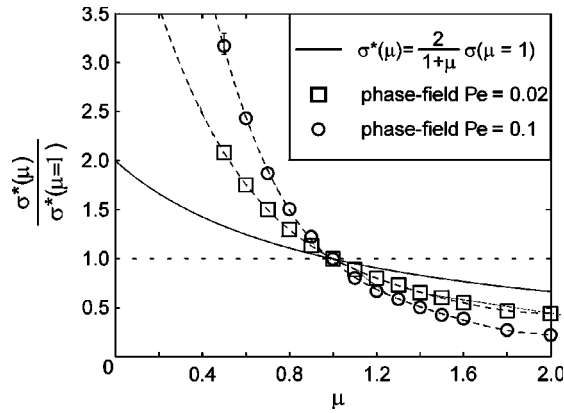


FIG. 1. The variation in  $\sigma^*$  [normalized against  $\sigma^*(\mu=1)$ ] as a function of  $\mu$  as predicted by our phase-field model for  $Pe=0.02$  and  $0.10$ . Also shown (solid curve) is the prediction of the analytical solvability model of Barbieri and Langer [15]. Note that where error bars are not shown this is because they are smaller than the plotting symbol used.

theory, the magnitude of that variation is significantly greater. Moreover, although the greatest departure is indeed at the higher undercooling studied, significant departures from the analytical model are seen even at the lower undercooling. These departures are most significant for  $\mu < 1$ . At  $\mu=0.5$  the variation in  $\sigma^*$  is 3.25 times that predicted by solvability theory at  $Pe=0.02$  and 6.5 times that predicted by solvability theory at  $Pe=0.10$ . For  $\mu > 1$ , which is the case corresponding to most metallic materials, the departures from the analytical theory are less extreme, although still significant. At  $\mu=2.0$  the variation in  $\sigma^*$  is 1.85 times that predicted by solvability theory at  $Pe=0.02$  and 2.5 times that predicted by solvability theory at  $Pe=0.10$ .

In order to ascertain whether the undercooling has a systematic effect on  $\sigma^*(\mu)$  and to establish whether there is a correspondence between our phase-field model and the work of Barbieri and Langer [15], the behavior of the derivative  $\partial\sigma^*(\mu)/\partial\mu$  in the vicinity of  $\mu=1$  has been studied. Values of  $\partial\sigma^*(\mu)/\partial\mu$  at  $\mu=1$  have been estimated numerically by running simulations at  $\mu=0.9, 1.0,$  and  $1.1$  over a wide range of undercoolings from  $\Delta T=75$  K ( $\Delta=0.17$ ) to  $\Delta T=400$  K ( $\Delta=0.92$ ). The variation in  $\partial\sigma^*(\mu, \Delta T)/\partial\mu$ , normalized against  $1/\sigma^*(\mu=1, \Delta T)$ , is shown in Fig. 2. It is found that, when plotted against  $\Delta T$ ,  $\partial\sigma^*(\mu, \Delta T)/\partial\mu$  is, to a very good approximation, linear, allowing extrapolation to the limit  $\Delta T \rightarrow 0$ . From Eq. (5) we have

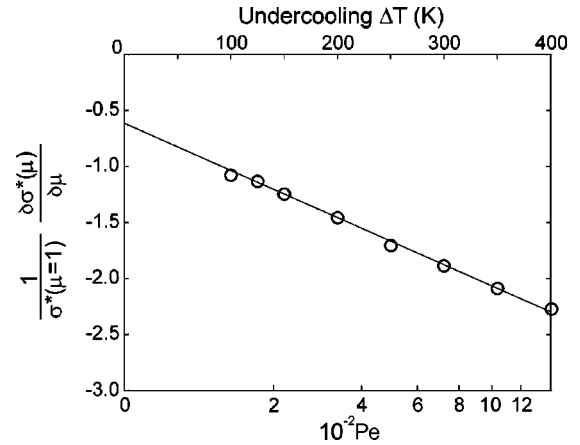


FIG. 2. The estimated derivative  $\partial\sigma^*/\partial\mu$  [normalized against  $\sigma^*(\mu=1)$ ] shown as a function of undercooling  $\Delta T$ . Note that extrapolation to the slow growth regime,  $\Delta T \rightarrow 0$ , yields a value close to  $-\frac{1}{2}$ , the value given by the solvability model of Barbieri and Langer [15].

$$\frac{1}{\sigma^*(\mu=1)} \frac{\partial\sigma^*}{\partial\mu} = \frac{-2}{(1+\mu)^2}, \quad (24)$$

which at  $\mu=1$  evaluates to  $-\frac{1}{2}$ , irrespective of  $\Delta T$ . From the figure it is clear that in the limit of  $\Delta T \rightarrow 0$  our estimate of  $[1/\sigma^*(\mu=1)][\partial\sigma^*(\mu)/\partial\mu]$  does indeed tend to a value close to  $-\frac{1}{2}$ , and consequently we would conclude that the analysis presented is not incompatible with the results of solvability theory. Any residual difference between our estimate in the limit  $\Delta T \rightarrow 0$  and the expected value of  $-\frac{1}{2}$  is probably a consequence of our simulation being run at finite  $\gamma$ . However, we would note that with regard to this particular effect significant departures from the results of solvability theory are encountered even at relatively modest undercoolings.

For reference, an undercooling of  $\Delta T=150$  K results in an estimated growth velocity of  $3.6$  m s $^{-1}$ , while at  $\Delta T=350$  K this figure is  $25$  m s $^{-1}$ . By way of comparison, undercoolings of  $350$  K can routinely be achieved in a range of metallic materials using containerless processing techniques and these large undercoolings result in very high growth velocities. In pure Cu, undercooled by  $336$  K, growth velocities as high as  $156$  m s $^{-1}$  have been recorded [25,26]. The results presented here should thus be borne in mind when using solvability theory to fit experimental data sets obtained from rapid solidification experiments.

- [1] D. P. Corrigan *et al.*, Phys. Rev. E **60**, 7217 (1999).  
 [2] U. Bisang and J. H. Bilgram, Phys. Rev. E **54**, 5309 (1996).  
 [3] G. P. Ivantsov, Dokl. Akad. Nauk SSSR **58**, 567 (1947).  
 [4] D. A. Kessler, J. Koplik, and H. Levine, Adv. Phys. **37**, 255 (1988).  
 [5] Y. Pomeau and M. Ben-Amar, *Solids far from Equilibrium* (Cambridge University Press, Cambridge, 1992), pp. 365–431.  
 [6] E. Brener and D. Temkin, Phys. Rev. E **51**, 351 (1995).

- [7] R. Kobayashi, Physica D **63**, 410 (1993).  
 [8] A. A. Wheeler, B. T. Murray, and R. J. Schaefer, Physica D **66**, 243 (1993).  
 [9] A. M. Mullis and R. F. Cochrane, Acta Mater. **49**, 2205 (2001).  
 [10] E. Brener, H. Muller-Krumbhaar, Y. Saito, and D. Temkin, Phys. Rev. E **47**, 1151 (1993).  
 [11] F. Marinuzzi, M. Conti, and U. Marini Bettolo Marconi, Phys. Rev. E **53**, 5039 (1996).

- [12] A. Karma and W. J. Rappel, Phys. Rev. Lett. **77**, 4050 (1996).
- [13] A. Karma and W. J. Rappel, J. Cryst. Growth **174**, 54 (1997).
- [14] A. Karma, Y. H. Lee, and M. Plapp, Phys. Rev. E **61**, 3996 (2000).
- [15] A. Barbieri and J. S. Langer, Phys. Rev. A **39**, 5314 (1989).
- [16] G. Busch, H.-J. Güntherodt, W. Haller, and P. Wyssmann, Phys. Lett. **43A**, 225 (1973).
- [17] W. Haller, H.-J. Güntherodt, and G. Busch, in *Liquid Metals 1976*, edited by R. Evans and D. A. Greenwood, IOP Conf. Ser. No. 30 (IOP, Bristol, 1977), p. 207.
- [18] Y. Ono and T. Yagi, Trans ISIJ **12A**, 314 (1972).
- [19] Y. Kita, M. Zeze, and Z. Morita, Trans ISIJ **22A**, 571 (1982).
- [20] T. Iida and R. I. L. Guthrie, *The Physical Properties of Liquid Metals* (Clarendon Press, Oxford, 1988).
- [21] S. E. Battersby, R. F. Cochrane, and A. M. Mullis, Mater. Sci. Eng., A **226**, 443 (1997).
- [22] S. E. Battersby, R. F. Cochrane, and A. M. Mullis, J. Mater. Sci. **34**, 2049 (1999).
- [23] S.-L. Wang, R. F. Sekerka, A. A. Wheeler, B. T. Murray, S. R. Coriell, R. J. Braun, and G. B. McFadden, Physica D **69**, 189 (1993).
- [24] A. M. Mullis, Acta Mater. **51**, 1959 (2003).
- [25] K. I. Dragnevski, R. F. Cochrane, and A. M. Mullis, Phys. Rev. Lett. **89**, 215502 (2002).
- [26] A. M. Mullis, K. I. Dragnevski, and R. F. Cochrane, Mater. Sci. Eng. (to be published).